

# GALILEO SIGNALS FOR SURVEYING AND MAPPING APPLICATIONS

Pedro F. Silva<sup>a</sup>, João S. Silva<sup>a</sup>, Tiago Peres<sup>a</sup>, José M. Palomo<sup>b</sup>,  
Ismael Colomina<sup>c</sup>, Christian Miranda<sup>c</sup>, M. Eulália Parés<sup>c</sup>, Chris Hill<sup>d</sup>,  
Paulo O. Camargo<sup>e</sup>, J. Moreira<sup>f</sup>, Gustavo Streiff<sup>g</sup>, Emerson Z. Granemann<sup>h</sup>, Carmen Aguilera<sup>i</sup>

<sup>a</sup> DEIMOS Engenharia S.A, Av. D. João II, Lote 1.17.01 – 10, Edifício Torre Zen, 1998-023 Lisboa, Portugal -  
(pedro.silva, joao.silva, tiago.peres)@deimos.com.pt

<sup>b</sup> DEIMOS Space S.L., Spain

<sup>c</sup> Institute of Geomatics, Spain

<sup>d</sup> University of Nottingham, UK

<sup>e</sup> UNESP, Brazil

<sup>f</sup> ORBISAT, Brazil

<sup>g</sup> MundoGEO, Brazil

<sup>h</sup> European GSA, Belgium

**KEY WORDS:** Galileo, AltBOC, GNSS, Hardware

## ABSTRACT:

The development of new GNSS systems, as the Galileo system (as well as the modernization of currently available ones, as the GPS) will provide additional signals with increasingly complex modulations and multiplexing schemes, enabling performance enhancements in terms of availability, accuracy, and robustness. The modulations to be used in the Galileo Open Service (OS) E1 and E5 signals shall enable much higher performances than the ones obtained with the current GPS civil signal (L1 C/A). Both Galileo E1 and E5 bands carry open OS wide-band signals, modulated with CBOC(6,1,1/11) and AltBOC(15,10) sub-carriers, respectively, that can be demodulated using techniques with different levels of complexity and accuracy. The Galileo E5 signal, with its Alternative Binary Offset Carrier (AltBOC) modulation, is one of the most advanced and promising signals of the Galileo system. Receivers capable of tracking this signal will benefit from unequalled performance in terms of measurement accuracy, precision, and multipath suppression. In the ENCORE project we are exploiting the ALTBOC signal's characteristics in order to generate the best possible pseudorange measurements, which when combined with E1 will allow for both mapping and surveying applications. In this paper we explain the main characteristics of these signals and present both theoretical and real results and how they can be used by the positioning algorithms to achieve a high accuracy solution which could have an impact in future applications.

## 1. INTRODUCTION

Taking benefit of the new Galileo ranging signals [1], the ENCORE (Enhanced Code Galileo Receiver) project is building a low-cost land management application, targeting the needs of the Brazilian market, using as baseline a low-cost Galileo Code Receiver. In particular, ENCORE explores the potential of E5 AltBOC and L1 MBOC Galileo signals for surveying applications based on pseudoranges, which allows high simplicity and robustness of data processing.

The use of GNSS in surveying relies on the use of high precision – mm level – carrier phase measurements to meet high position precision requirement, while pseudorange measurements are used for various cadastral, GIS and mapping applications with meter and lower level accuracy requirements. The main advantages of pseudorange positioning are the simplicity and robustness of data processing, reduced mapping gear and less GNSS education and training than the typical GNSS geodetic surveyor.

However, there are cadastral and mapping applications that require better accuracies than current pseudoranges measurements provide and there are surveying applications that do not require the cm level accuracies that carrier phase measurements provide. Hence receivers are either too expensive

(receivers, processing software, additional hardware infrastructure, trained personnel) or unacceptably inaccurate. This gap can be reduced or eliminated with the new GPS and Galileo signals (described in [1], [2], and [3]).

A solution for low cost and high accuracy mapping would provide significant benefits, specially in the case of countries such as Brazil, where there is currently a significant demand for property surveying. Additionally, the characteristics of Galileo signals could also be exploited in more challenging environments such as users in urban scenarios in applications such as GIS and mapping.

According to theoretical results, pseudoranges can be extracted from the Galileo E5 AltBOC signals with tracking errors ( $1-\sigma$ ) ranging from 0.02 m (“open sky” scenarios) to 0.08 m (“tree covered” scenarios with 15% through-foliage visibility) whereas for the Galileo E1 CBOC signals the tracking errors range between 0.25 m and 2.00 m respectively. These values have been experimentally confirmed with ENCORE receiver using synthetic IF signals. With these tracking errors and with the explicit estimation of the ionosphere parameters, the available simulations indicate “open sky” horizontal/vertical positioning precisions of 3-10 cm and 3-20 cm for (low dynamics) kinematic positioning.

Absolute positioning surveying is likely to emerge as a standard procedure, both in real-time (using broadcast orbits or ultra-rapid ones hopefully available in the future from the IGS, [4]) or in post-processing (similarly, using precise Galileo orbits). Absolute pseudorange positioning is of particular interest because simple GNSS surveying with pseudoranges can become a practical tool in regions with sparse GNSS permanent station distributions and for communities with limited surveying expertise.

The ENCORE project is being performed in the frame of the 7th Framework Programme under European GNSS Supervisory Authority (GSA) co-funding, where DEIMOS Engenharia is leading the European-Brazilian consortium. The consortium brings together technological companies, application dealers, research centres, universities and geoinformation providers, involving all key actors for successful demonstration of ENCORE potential. The application of the ENCORE receiver in urban environments is also under study in the RXURB (Hybrid Code Receiver for Urban Navigation) project, funded under the Portuguese QREN initiative.

This paper is organized in six main sections. The current introduction is followed by an overview of the regional context in Brazil. The third section describes the Galileo signals of interest in this project followed by a fourth section describing the overall system and test setup. The fifth section provides an overview of the main algorithms (signal processing and positioning), followed by the results section with for code tracking and positioning performance results. The main conclusions of the work are presented in the sixth section.

## 2. SUMMARY OF REGIONAL CONTEXT

The Brazilian system of property registration, which is based in the German model, establishes that only those who register a property are entitled to its ownership. In such system, each property has a record comprising its history, which guarantees safer estate transactions. With the introduction of Law 10.267/01 [5], the register includes a technical record in a single database. Information such as coordinate of the vertices defining the property, georeferenced to Brazilian Geodetic Frame (BGF) is included in the record.

Not only does Law 10.267/01 fights land-grabbing operations and the illegal formation of latifúndios (large portions of land belonging to a single land owner), but it also creates a rural technical record, which is a great advance in the Brazilian cartography record because it generates a geo-referenced territorial database, a tool of key importance for the country's territorial management, planning and development.



Figure 1. Dual frequency receiver data collection setup in Brazil

In early 2010, only 0,2% of the total number of Brazilian properties had been geo-referenced and certified by INCRA. It can be verified that the period of time established for geo-referencing is unlikely to be met and extensions to the time periods are likely required.

The cost of equipment and difficulties faced by landowners and the delay of INCRA in the certification of properties, amongst other factors are important causes that prevent professionals to perform the work at accessible prices to the owners. It also reduces the number of professionals acting in geo-referencing.

Taking benefit of Galileo signal characteristics (such as the multipath robustness and code observables precision of the AltBOC signal), the production of robust GNSS receivers at a low cost will allow more professionals to act in the geo-referencing of rural properties, surveillance and demarcation of permanent reservation areas and legal reserve (see Figure 1). This will also allow that the geo-referencing of rural properties and the environmental legalization be carried out in a shorter time.

## 3. TARGET GALILEO SIGNALS

The development of new GNSS systems, as the Galileo system [1] (as well as the modernization of currently available ones, as the GPS) will provide additional signals with increasingly complex modulations and multiplexing schemes, enabling performance enhancements in terms of availability, accuracy, and robustness. Figure 2 shows the current and future GPS and Galileo bands.

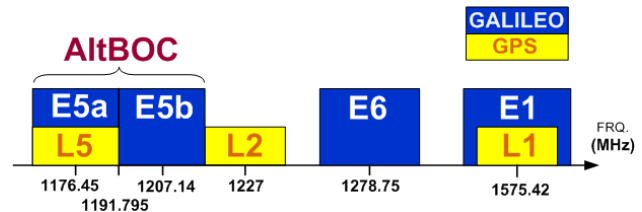


Figure 2. Spectrum of current and future GPS and Galileo signals

Performance of GNSS receivers in terms of tracking noise and multipath robustness are closely related to the slope of the main peak of the signal's Auto-Correlation Function (ACF) as well as its overall shape. A steeper main peak translates into lower tracking noise and higher multipath robustness while more secondary peaks also improve multipath robustness. The most recent optimization of signals for satellite navigation has shown a trend towards increasing the spectral occupancy (see Figure 3), in order to obtain signals that provide ACFs with steeper peaks.

shows the ACFs for the most relevant GPS and Galileo modulations and shows the multipath error envelopes for the corresponding GPS and Galileo signals when using a Early-Late Power discriminator and a correlator spacing of 0.1 chip (assuming one reflected ray and a carrier over a multipath ratio of 2).

The modulations to be used in the Galileo Open Service (OS) E1 and E5 signals shall enable much higher performances than the ones obtained with the current GPS civil signal (L1 C/A).

The proposed Enhanced Galileo Code Receiver (ENCORE) will harvest the potential of the Galileo signals to generate the best possible pseudorange measurements (which are the inputs of the positioning algorithms).

Both Galileo E1 and E5 bands carry open OS wide-band signals, modulated with CBOC(6,1,1/11) and AltBOC(15,10) sub-carriers, respectively, that can be demodulated using techniques with different levels of complexity and accuracy.

Multiplexed BOC (MBOC) is a new modulation introduced in 2006 [6], and included recently in the Galileo SIS ICD [1]. The E1 Open Service modulation receives the name of Composite Binary Offset Carrier (CBOC) and is a particular implementation of MBOC. The CBOC(6,1,1/11) modulation is the result of a linear combination of a wideband BOC(6,1) sub-carrier with a narrow-band BOC(1,1) sub-carrier, in such a way that 1/11 of the power is allocated (in average) to the high frequency component.

Nevertheless, the potential of the future Galileo E5 signal is expected to outshine even these modernized signals. The Galileo E5 signal, with its Alternative Binary Offset Carrier (AltBOC) modulation [7], is one of the most advanced and promising signals of the Galileo system. Receivers capable of tracking this signal will benefit from unequalled performance in terms of measurement accuracy, precision, and multipath suppression [8]. However, the signal processing techniques to implement a matched-filter AltBOC demodulation are much

more challenging than those for the traditional BPSK or even for the BOC and CBOC modulations. This stems from the large bandwidth (chip rate), complex sub-carrier, elaborate multiplexing scheme (which enables the simultaneous broadcast of 4 channels on a single carrier) and complex interaction of the 4 multiplexed channels [7].

The AltBOC(15,10) correlation peak is similar to the one of BOC(15,10) near the main peak and, as suggested in [7], it outperforms all other modulations of the current and future GPS and Galileo civil and open service signals (note that the x axis of [7] is also normalized by the chip period, which is 10 times shorter for the AltBOC(15,10) modulation than for the remaining ones).

In the absence of multipath or signal fading sources, the preliminary performances achievable with E5 AltBOC and E1 CBOC in terms of accuracy of the code tracking errors is 0.02 m and 0.25 m respectively at 45 degree (about 40 dB-Hz for E1 and 44 dB-Hz for E5) with a correlator spacing of 0.1 chip and integration times of 4 ms. Figure 6 illustrates the theoretical code errors v.s. C/N0 for the AltBOC(15,10) and CBOC(6,1,1/11) signals and their dual frequency (iono-free) combination. As it can be seen in Figure 6, the iono-free combination does not benefit from the low noise properties of AltBOC, on contrary to the solution proposed in ENCORE (see the algorithms section of this paper).

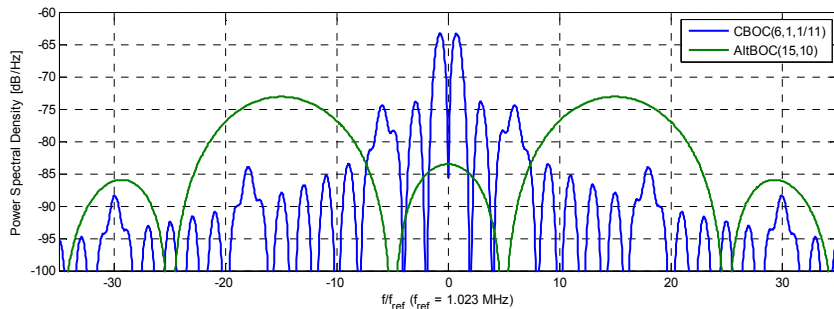


Figure 3. Watt Normalized PSD of MBOC(6,1,1/11) and AltBOC(15,10) (transmitted over infinite bandwidth)

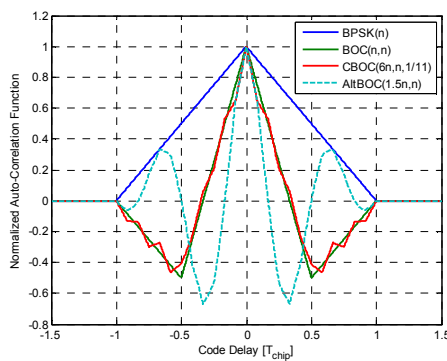


Figure 4. Normalized auto-correlation functions for different modulations: BPSK (n) of GPS L1, BOC (n,n) of Galileo E1 with simplified demodulation, CBOC(6n,n,1/11) of Galileo E1, and AltBOC(1.5n,n) of Galileo E5 signals.

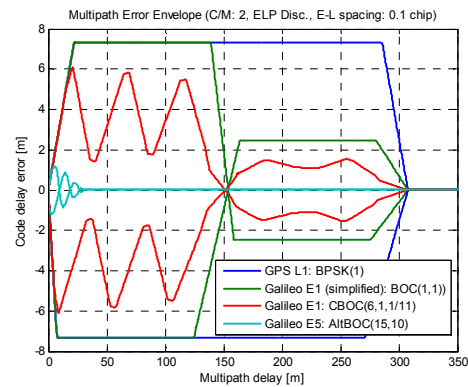


Figure 5. Multipath error envelopes for GPS L1, Galileo E1 (demodulated as BOC(1,1) and CBOC(6,1,1/11)), and Galileo E5 signals (Early-Late Power discriminator, correlator spacing of 0.1chip, carrier over multipath ratio of 2 and infinite bandwidth).

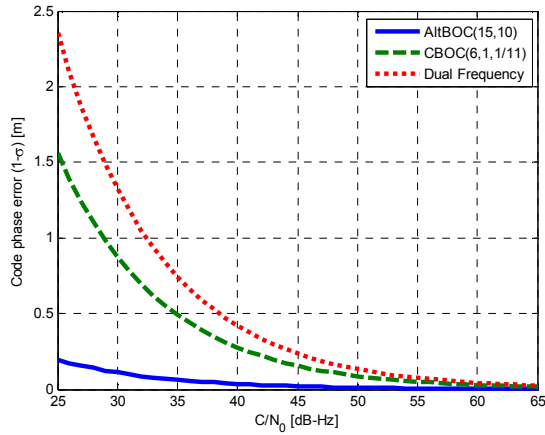


Figure 6. Theoretical code measurement noise comparison between BOC and AltBOC

If multipath and signal fading sources are present, the expected errors increase to 0.08 m and 2 m respectively (for about 36 dB-Hz for E1 and 40 dB-Hz for E5). Longer integration times will lead to better performances.

During the project, theoretical results will be compared against those obtained with Galileo live signals and in the current paper we provide results obtained with Galileo synthetic signals.

#### 4. SYSTEM DESCRIPTION AND TEST PLATFORM

The ENCORE system can be divided in two main components: the ENCORE Code Receiver and the ENCORE Application Software.

The ENCORE Code Receiver, shown in Figure 7, consists of the Antenna, the RF Front-End (Figure 8), and the Baseband Signal Processing Core. The Code Receiver can be enclosed in a host computer platform on which the ENCORE Application Software will be operating.

The ENCORE Application Software is responsible for the data processing and visualisation to the end-user as well as execution of the positioning algorithms to support the data processing. The application runs on a portable or Desktop Computer and interfaces the ENCORE Code Receiver using a TCP/IP connection for the retrieval of necessary data for real-time and post-processing determination of the receiver positioning solution.



Figure 7. ENCORE Code Receiver under testing

#### 4.1 Code Receiver

The ENCORE Code Receiver builds upon existing receiver core modules (implemented on FPGA) available from past projects and to which an Antenna and a dual-frequency (E1+E5) RF Front-End (developed by ORBISAT in the scope of the ENCORE project) were added. A description of the ENCORE Code Receiver's hardware modules is given below.

##### 4.1.1 Antenna and RF Front-End

The RF Front-End, which processes the signals received by an Active Antenna, is composed of two main blocks: a dual-frequency RF Converter and an Analog-to-Digital Converter (ADC). Figure 8 shows the prototypes of the RF Converter and the ADC as well as their connection.

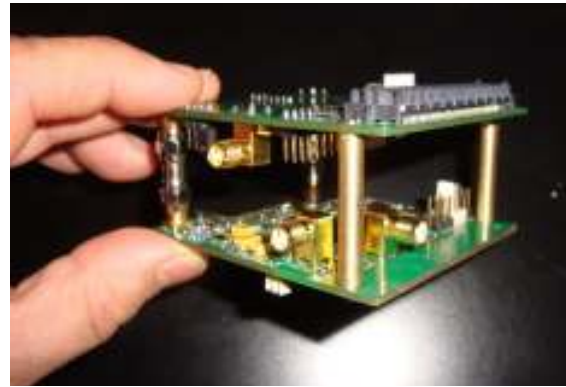


Figure 8. Dual-frequency RF Converter (bottom) connected to ADC (top)

The RF Converter is responsible for down-converting the signal at the E1 band to a band centred at 70 MHz and the signal at the E5 band to a band centred at 140MHz, which are the system IF bands. The IF-signals are then sampled at 185,625 MHz and digitalized by an 8-bit ADC. The digital signals are made available to the Baseband Signal Processing core through an FMC connector (top right of Figure 8). A standard expansion header also provides access to the signals for testing purposes.

##### 4.1.2 Baseband Signal Processing Core

The Baseband Signal Processing Core is implemented on a Field-Programmable Gate Array (FPGA) platform, which hosts both the DSP cores and microprocessor on which the receiver firmware is running.

The architecture of the Baseband Signal Processing Core is depicted in Figure 9, in which the following cores can be highlighted:

- The Input Modules (IM), where the incoming signals are converted to baseband, filtered and re-quantized;
- The GNSS Channels, which are responsible for the GNSS baseband signal processing: carrier and code spreading and samples accumulation;
- The Ethernet MAC and the PCIE Controllers, which allow communications via Ethernet and/or PCIE bus, respectively;
- The Microblaze Processor, an embedded micro processor on which the receiver firmware runs.



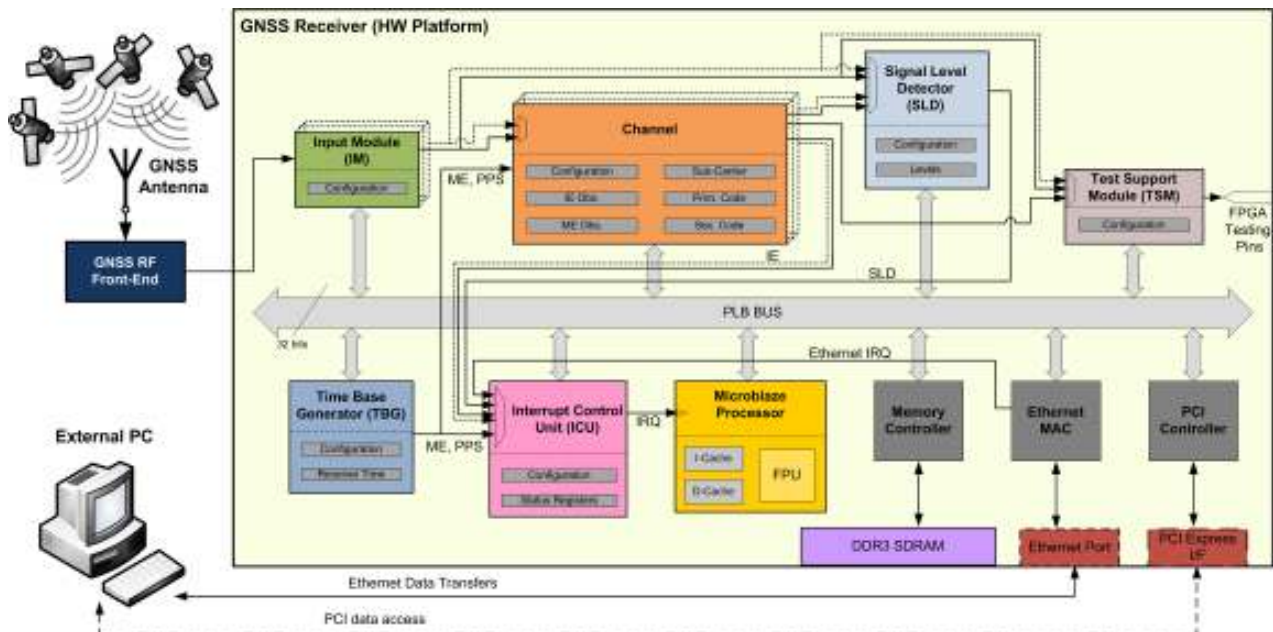


Figure 9. Dual Receiver Hardware Components and Interfaces

## 4.2 Application Software

The Application Software's main objective is to interface the receiver (to allow the retrieval of live or collected data) and process and/or visualize the data/results (either in real-time or post-processing). It runs on a Desktop computer under MS Windows environment and the programming environment is based on Java for improved software portability. The main functionalities are the following ones:

- Processing of data collected by the receiver and generating the position solution. Depending on the operating mode and the desired accuracies, the processing can be performed in real-time or in post-processing according to user configuration options;
- Importing and storing files, where data from the receiver or other sources is imported for subsequent processing or stored in real-time if the software is connected to the receiver. RINEX data conversion is also supported;
- Results visualisation and report generation, where the navigation solutions are displayed and formatted into the appropriate output structure for later access. It allows visualisation of the evolution (with time) of satellite ID,  $C/N_0$ , elevation angle, observables and position error statistics, among other information.

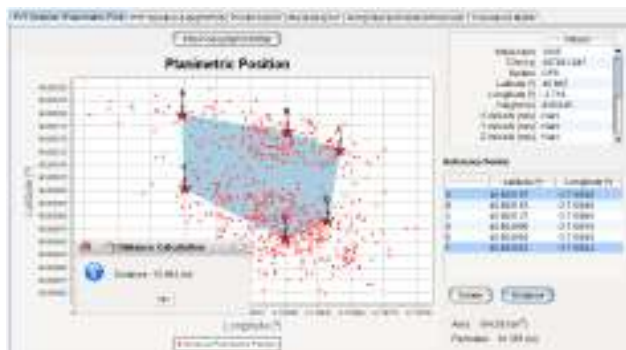


Figure 10. Application software graphical user interface - area and perimeter visualisation example

Figure 10 illustrates the application software determining the area and perimeter using several position points collected by the receiver.

Although the receiver is a dual frequency one, the positioning algorithm won't be based on ionospheric-free combination, as it would eliminate the low noise properties of E5 AltBOC. The implemented algorithm follows a PPP approach, as described in the next section.

Accuracies of at least 0,50 m (1) are targeted for Real-Time operation although higher accuracies are expected to be achieved in post-processing (preliminary analysis [9] indicated that positioning accuracies of 20 cm can be achieved), addressing the widest possible number of receiver surveying classes described in [10]

## 5. ALGORITHMS

The following sections present the algorithms implemented on the ENCORE system in terms of signal processing and positioning.

### 5.1 Baseband Signal Processing

A dual-frequency configuration was considered necessary, taking into account the targeted accuracies and the need to mitigate ionospheric effects. Therefore, both AltBOC and CBOC signal processing architectures were analyzed. However, there are a number of different receiver architectures that can be used to process each of the target signals, differing mainly in terms of complexity and achievable accuracy and sensitivity.

The Galileo CBOC(6,1,1/11) signal's demodulation can be simplified by using a BOC(1,1) modulated local replica, at the expense of tracking and multipath robustness performance (making it comparable to that of a BOC(1,1) signal) but enabling an interesting trade-off between performance and receiver complexity.

As for the E5 signal, it can be separated into two sub-bands (E5a and E5b) which can be treated separately by a Galileo E5 receiver (as BPSK(10) modulated signals), called Single Side-Band (SSB) processing. However, this would result in the loss of the promising AltBOC signal properties (resulting in a classical triangular ACF). A matched filter demodulation of the full Galileo E5 signal is required to implement the best possible receiver in terms of accuracy and multipath robustness, at the expense of an increase in the receiver complexity and required bandwidth.

Therefore, in the design stage of the ENCORE Code Receiver, different architectures for each of the Galileo E1 CBOC and E5 AltBOC signals were analyzed taking into account the following factors:

- Support (in terms of HW signal processing structures) for both E1 and E5 signals (taking into account their complex modulations and the existence of pilot and data signals);
- Maximization of the use of the potential of the signals in terms of accuracy and multipath robustness;
- HW complexity and resource requirements;
- Pre-existing developments in terms of receiver signal processing cores;
- Flexibility (architecture upgradeability with minimum HW impact).

### 5.1.1 Galileo E5 AltBOC Signal Processing

Six different approaches/architectures for the processing of the Galileo E5 AltBOC signal were analysed with respect to tracking noise and multipath robustness:

- A Single Side-Band (SSB) tracking approach, in which the E5a and E5b sub-bands are processed independently (as BPSK(10) signals), and which fails to harvest the full potential of the AltBOC signal;
- Two AltLOC approaches (one with pilot tracking only and another one with pilot tracking plus data demodulation), which are an alternative to the AltBOC approach in which a linear sub-carrier is used instead of the digital AltBOC sub-carrier;
- Two AltBOC approaches (one with pilot tracking only and another one with pilot tracking plus data demodulation);
- A full AltBOC approach (with the tracking of all four channels, which also served as reference).

Taking into account that data demodulation is required for the navigation message recovery (needed for positioning and for corrections calculation), a technique which allows data demodulation was found necessary, excluding pilot-only approaches. Additionally, to track weak signals and/or to perform long integrations to improve measurement quality, pilot tracking was found to be necessary, excluding data-only approaches. Therefore a pilot tracking approach which supports data demodulation was selected (the complexity increase of processing both pilot and data channels was limited by including only 1 extra correlator for each data component).

To harvest the multipath mitigation potential of the AltBOC modulation, SSB tracking was excluded.

Finally, to avoid different architectures for AltBOC and CBOC signals, the AltBOC approach was preferred w.r.t. the AltLOC one.

Taking all the above into account, the AltBOC pilot tracking + SSB data demodulation approach was selected for implementation.

### 5.1.2 Galileo E1 CBOC Signal Processing

Four different approaches/architectures for the processing of the Galileo E1 CBOC signal were analysed with respect to tracking noise and multipath robustness:

- A CBOC code replica approach, in which the local code replica is CBOC(6,1,1/11) modulated;
- A simplified approach, in which the local code replica is BOC(1,1) modulated;
- The TM61 approach [13], in which the local code replica is modulated by a TMBOC signal;
- The Dual Correlator technique [13] (based on the fact that the CBOC sub-carrier is a linear combination of two BOC sub-carriers), in which there are two local replicas, modulated with BOC(1,1) and BOC(6,1) signals, and the correlator outputs are linearly combined, producing outputs that are equivalent to those if a CBOC modulated local code was used.

The techniques which provide the best tracking performance are the matched filter CBOC code replica approach and the Dual Correlator Technique (which simulates it in SW), the later requiring more hardware resources and computational power than the former.

Although the complexity of the CBOC code replica approach is high, since the AltBOC pilot tracking + SSB data demodulation approach was selected for E5 signal processing, the structures needed to support the CBOC approach are already required (as well as the processing power to handle high BW signals). Therefore, the CBOC code replica approach was selected.

## 5.2 Positioning Models and Algorithms

The observation equations for pseudorange measurements follow the modelling principles of PPP. Thus, the observed pseudoranges  $P_{1r}^s$  (E1 CBOC) and  $P_{5r}^s$  (E5 AltBOC) can be modelled as

$$P_{ir}^s = \rho_r^s + c(\delta t^s - \delta t_r) + R^s + (T_r^s + \delta T_r^s) + \frac{I_r^s + \delta I_r^s}{f_i^2} + c(b_i^s - b_{ir}) \quad (1)$$

where  $i = 1, 5$  is refers to the E1 or E5 signals  
 $\rho_r^s$  is the true geometric distance between satellite  $s$  and receiver  $r$   
 $c$  is the speed of light in a vacuum  
 $\delta t^s$  is the given  $s$  satellite clock correction  
 $R^s$  is the relativistic “correction” for satellite  $s$   
 $T_r^s$  is the modelled or given tropospheric delay  
 $f_1, f_5$  are the frequencies of E1 CBOC and E5 AltBOC signals, respectively  
 $I_r^s / f_i^2$  are the modelled or given ionospheric delays  
 $b_i^s$  are the given biases for satellite  $s$ .

In the above pseudorange observation equation we will estimate the receiver position  $X_r$  (included in  $\rho_r^s$ ), the receiver clock correction  $\delta t_r$ , the correction  $\delta T_r^s$  to the modelled or given

tropospheric delay  $T_r^s$ , the term  $\delta I_r^s$  related to the correction  $\delta I_r^s/f_i^2$  to the modelled or given ionospheric delays  $I_r^s/f_i^2$ , and the receiver frequency dependent biases  $b_{i,r}$ . In equation 1,  $\rho_r^s$  is a well known function of the satellite ephemeris, the receiver position, the satellite and receiver antenna phase centre offsets, and of all the effects, like solid Earth tides, usually included in PPP models.

The time dependent unknown parameters in equation 1 are further modelled as random walk stochastic processes for the stochastic differential equation of the prediction step (Kalman filter estimation approach) or of the dynamic model (dynamic network estimation approach [11]), as follows [12]:  $\delta t_r$  is a random walk with rather large driving white noise variance [rw ( $\infty$ )];  $\delta T_r^s$  as rw ( $0.015^2 \text{ m}^2$ ), PSD level;  $b_{i,r}$  as rw ( $0.0017^2 \text{ m}^2$ ), PSD level ( $b_{1,r}$  is set to 0); and  $(I_r^s + \delta I_r^s)/f_i^2$  as rw ( $\sigma^2 \text{ m}^2$ ) with

$$\sigma^2 = \frac{\sigma_\infty^2}{2} \left(1 - e^{-2|\tau|/T}\right) \quad (2)$$

where  $\sigma_\infty^2 = 2 \text{ m}^2$   
 $T = 64 \times 60 \text{ s}$   
 $\tau$  is the time interval (in seconds) between two successive measurements.

Clearly, the stochastic model for the total ionospheric delay depends on assumptions for  $\sigma_\infty$  and  $T$  that also depend on the solar activity. Furthermore, depending on the model or data used for  $I_r^s$  the actual parameter to be estimated  $\delta I_r^s$  and, specifically  $\delta I_r^s/f_i^2$ , will obey to different “amplitude”  $\sigma_\infty$  and “time correlation”  $T$  values. For the results reported in the paper, the three-dimensional, time dependent ionospheric electron density NeQuick model was used for  $I_r^s$ . For  $\delta I_r^s/f_i^2$ , the values  $\sigma_\infty^2 = 0.3 \text{ m}^2$ ,  $T = 5 \times 60 \text{ s}$  were adopted.

In the ENCORE project, the above models are used to investigate the performance of the various positioning modes (absolute and relative, static and kinematic, as depicted in Figure 11) and procedures (with and without a “ground pre-surveyed” or “ground control” point in the absolute positioning mode).

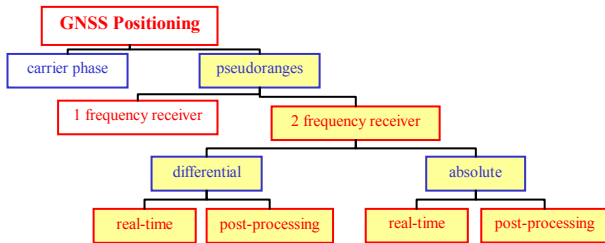


Figure 11. The 4 positioning modes in ENCORE

## 6. RESULTS

### 6.1 Tracking Results

This section presents the first results of the integration tests. For these tests, the GNSS receiver was fed with synthetic E1 CBOC

and E5 AltBOC signals with different powers. The receiver’s configuration used for E1 and E5 signals is shown in Table 1.

Parameters	Values	
Signal	E1 MBOC	E5 AltBOC
Integration period [ms]	4	1
E-L spacing [chip]	0.0853	0.1705
Code discriminator	E-L Power	
Code loop bandwidth [Hz]	1	
Carrier discriminator	Q/I	
Carrier loop bandwidth [Hz]	4	
Pre-correlation sampling frequency [MHz]	120	

Table 1. Receiver configuration

#### 6.1.1 E1 MBOC Tracking Results

Figure 12 shows the code phase tracking error evolution for E1 MBOC signal with carrier-to-noise density ratio,  $C/N_0$ , of 46.6 dB.Hz. The histogram with the code error values distribution is plotted in Figure 13. As it can be seen, the maximum error doesn’t exceed 0.5 m and the majority of the values fall inside the 20 cm error window.

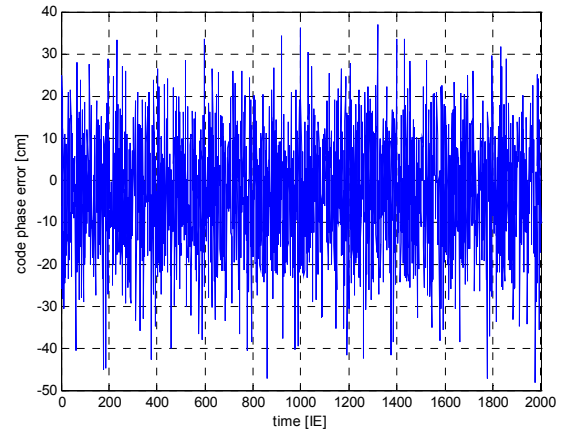


Figure 12. Code phase tracking error for E1 MBOC signal with  $C/N_0 = 46.6 \text{ dB.Hz}$

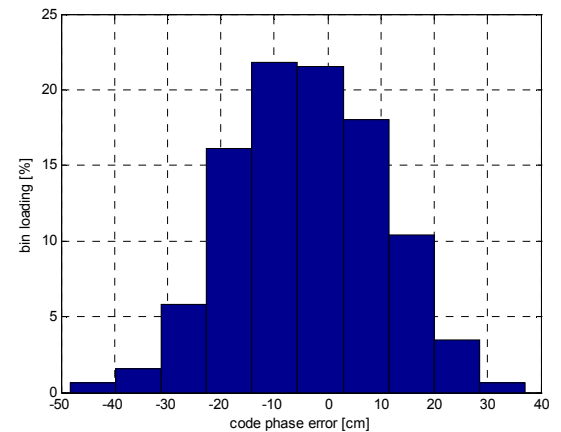


Figure 13. Histogram of the code phase tracking error for E1 MBOC signal with  $C/N_0 = 46.6 \text{ dB.Hz}$

Figure 14 and Table 2 show the measured and the theoretical [8] code phase tracking errors (1-sigma) for E1 MBOC signal and three different  $C/N_0$  values. The measured values are above

the theoretical ones, but have the same order of magnitude. It must be noted that for all the  $C/N_0$  values sub-meter precision was reached.

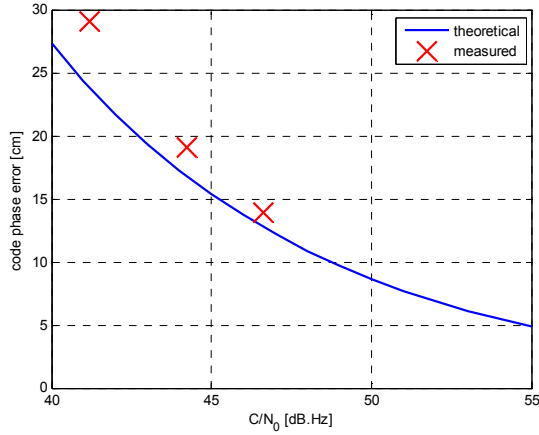


Figure 14. Measured and theoretical code phase tracking error for E1 MBOC signals

$C/N_0$ [dB.Hz]	Code Phase Tracking Error [cm]	
	Measured	Theoretical
46.6339	13.8647	12.6777
44.2430	19.0721	16.7534
41.2091	29.0494	23.7578

Table 2. Measured and theoretical code phase tracking error for E1 MBOC signals

### 6.1.2 E5 AltBOC Tracking Results

Figure 15 and Figure 16 show, respectively, the code phase tracking error evolution and histogram for an E5 AltBOC signal with  $C/N_0 = 50.1$  dB.Hz. It should be highlighted that the maximum code error is roughly 2 cm and that the majority of the error values are below 1 cm. The measured cm-level precision demonstrates the advantages of the E5 AltBOC signal, with the code tracking error being one order of magnitude lower than the one obtained with E1 signals.

The measured code phase tracking errors for E5 AltBOC signals are compared with the theoretical ones [8] in Table 3 and in Figure 17.

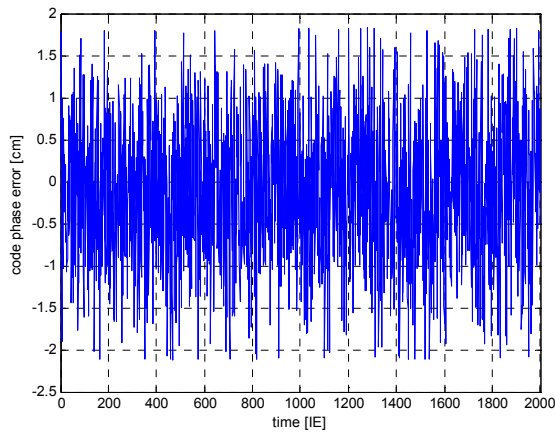


Figure 15. Code phase tracking error for E5 AltBOC signal with  $C/N_0 = 50.1$  dB.Hz

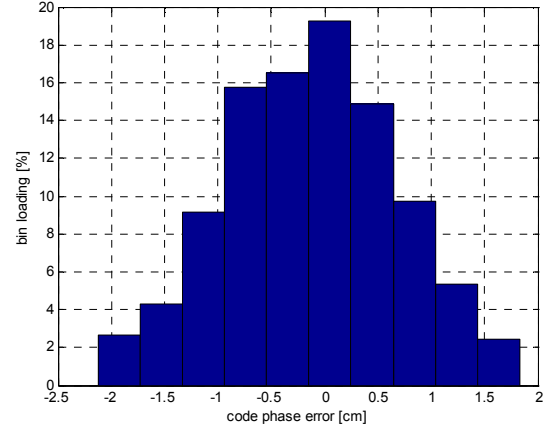


Figure 16. Histogram of the code range error for the E5 AltBOC signal with  $C/N_0 = 50.1$  dB.Hz

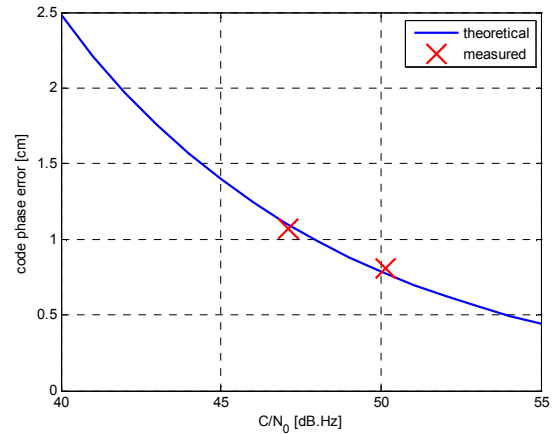


Figure 17. Measured and theoretical code phase tracking error for E5 AltBOC signals

The measured values are inline with the theoretic values. Once more, it should be highlighted that the precision is within the order of magnitude of 1 cm, for the  $C/N_0$  values tested, which support the usefulness of the new Galileo E5 signals.

$C/N_0$ [dB.Hz]	Code Phase Tracking Error [cm]	
	Measured	Theoretical
50.1382	0.80979	0.77323
47.1022	1.0736	1.0967

Table 3. Measured and theoretical code phase tracking error for E5 AltBOC signals

## 6.2 Positioning Results

This section presents the latest results of the positioning algorithms tests. The four positioning methods (described in the Algorithms section) and two procedures are being investigated [9].

The criteria used to define the test scenarios was that they should be as realistic as possible and correspond to a partial deployment of the Galileo constellation (18 satellites expected by 2015). Due to the unavailability of sufficient Galileo space vehicles at the moment, the validation of the algorithms described before was done by feeding the positioning



algorithms with data generated using the Navigation Sensor Simulation (NSS) tool, developed by University of Nottingham. The NSS data simulation tool was originally designed to simulate the types of measurements that can be made using a GNSS receiver. Specifically the simulator has the capability of producing code, carrier and Doppler measurements on L1, E1, E5a, E5b, E5 (combined), L2c, L5 and E6 frequencies, covering GPS and Galileo systems.

The simulated data is based on the true locations of both the receiver and the satellites to calculate the true, error-free measurements. Error models are then applied to account for the various inaccuracies seen in real-world measurements. The simulation results are returned to the user in a file in the standard Receiver Independent Exchange (RINEX) observations format. The parameters used for the simulation of the scenarios was presented in [9].

Table 3 contains a summary of the results of the positioning and receiver clock determination time series for epoch 301 to epoch 3600 after allowing 5 minutes – epochs 1 to 300 – for filter convergence. Each table row contains the estimated means and standard deviations of the differences between the solution time series and the true value of the point coordinates and receiver clock corrections. In the case of the test cases K-16 and K-21, this describes the empirical accuracy and precision of kinematic positioning as data were processed in the kinematic mode. In the cases S-16 and S-21 these differences indicate the potential accuracy and precision of static positioning.

In all cases, the results are excellent and indicate horizontal precisions at the cm-level, from 1 cm to 3 cm, and vertical precisions at the dm-level, from 5 cm to 25 cm. Accuracy is at the dm-level, with error means ranging from -16 cm to 12 cm for the horizontal components and from -36 cm to 39cm for the vertical component.

Test	ENh (m)						clock (m)	
	$\mu_E$	$\mu_N$	$\mu_h$	$\sigma_E$	$\sigma_N$	$\sigma_h$	$\mu$	$\sigma$
S-16	-0.16	0.12	-0.36	0.02	0.03	0.06	0.52	0.06
K-16	-0.13	0.10	-0.36	0.02	0.03	0.25	0.54	0.18
S-21	-0.14	0.12	0.29	0.03	0.01	0.11	0.16	0.35
K-21	-0.12	0.12	0.18	0.02	0.03	0.14	0.20	0.36
average no. of satellites: 5.8 (S-16, K-16), 6.1 (S-21, K-21)								

Table 4. Empirical results (errors) of point positioning for the E1/E5combination

The results in Table 3 are illustrated with the corresponding graphics for the test cases S-16 (Figure 18 through Figure 20) and K-21 (Figure 21 through Figure 23).

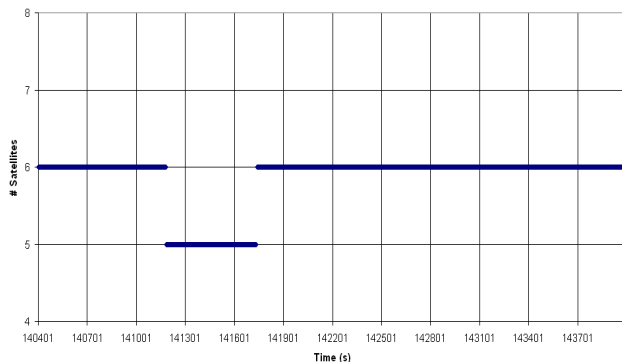


Figure 18: Number of satellites for test case S-16.

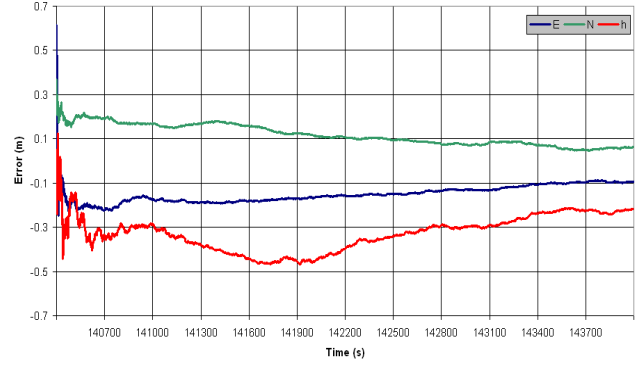


Figure 19: Position accuracy for test case S-16.

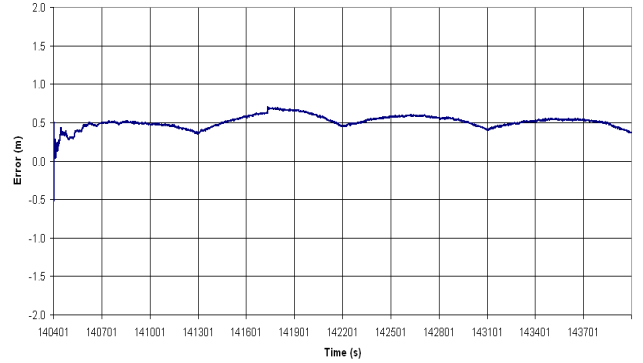


Figure 20: Receiver clock accuracy for test case S-16.

In the S-16 case, besides the impact of the 600 s period with just five satellites on the height component, a rather smooth behavior can be identified in the three components. The effect of the orbit and satellite clock errors is clear on the systematic error and a slow “convergence” to the true values seems to happen. We believe that the “convergence” is rather a slow absorption of the orbital and clock errors by other unknowns than a Kalman filter convergence effect as shown by the stability of the clock corrections. On the other side, the receiver clock corrections exhibit a periodic (900 s) behavior that may be related to the frequency and interpolation of the orbits but which is not fully understood yet.

The K-21 case, being it a kinematically processed data set, shows a noisier behavior than S-16. The 60 s initial static period at a point of known coordinates can be clearly recognized. Were it not for the missing satellite in the S-16 case, the error behavior of K-21 would be very similar – just noisier – to S-16.

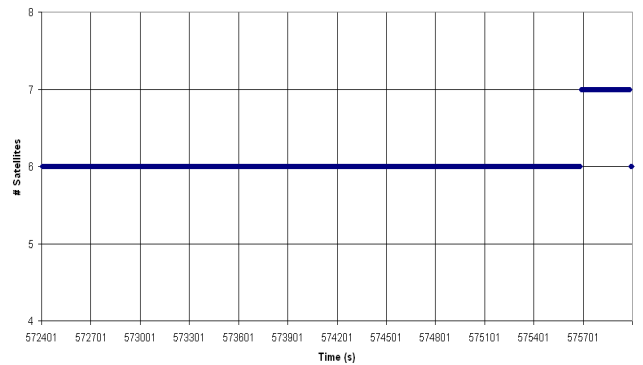


Figure 21: Number of satellites for test case K-21.

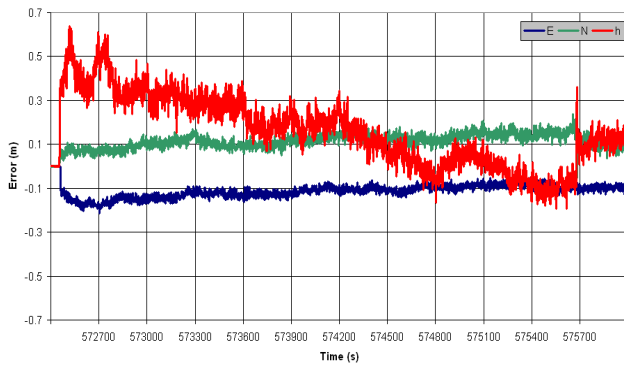


Figure 22: Position accuracy for test case K-21.

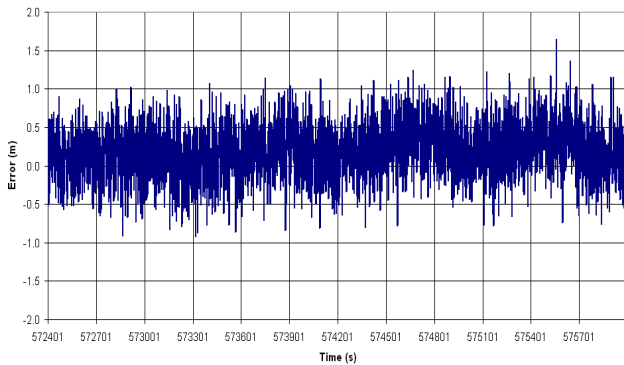


Figure 23: Receiver clock accuracy for test case K-21.

It is interesting to see how an additional seventh satellite in the last 60 s helps in reducing the systematic vertical error. Like the S-16 case, the influence of broadcast orbits and the fact that no backward Kalman filtering and smoothing was used plays against the accuracy and precision of positioning.

## 7. CONCLUSIONS

A tool for surveying and mapping applications (targeting land management applications in the Brazilian context) is being developed in the scope of the ENCORE project, taking advantage of the novel Galileo signals' characteristics (AltBOC and CBOC modulations) and based on a low-cost code-only approach. A receiver prototype, consisting of a custom-made RF Front-End, an FPGA, innovative signal processing algorithms (running on a soft-processor on the FPGA), dedicated positioning algorithms, and an application software (with a graphical user interface) has been developed and implemented and is currently undergoing final tests.

An extensive test campaign, involving the integration an system test of the ENCORE receiver with of real and synthetic data and currently ongoing, shall support the validation of previous simulation results and the demonstration of the applicability of the proposed concept to the target application. This paper presents the first set of results of the formal ENCORE test campaign (which shall continue over the next few months and include tests with live Galileo signals), showing performances within the specified requirements. The presented results are related with two types of tests: (code) tracking tests, which focused on the performance of the receiver's code tracking loops, and positioning tests, which focused on the accuracy of the positioning solution.

Code tracking precisions of about 13 cm for E1 and 1 cm for E5 (for  $C/N_0$  of approximately 47 dB-Hz) have been achieved with the ENCORE prototype during the tracking tests (in which synthetic IF signals were fed to the receiver prototype). These results were inline with the expected results, obtained in preliminary analyses [9], in which tracking precisions of about 0.25 m for E1 and 2 cm for E5 were expected under "open sky" and conditions.

Positioning performance results of the proposed combined Galileo E5/E1 and parameter estimation approach (discussed in [9]) in a real-time scenario (using broadcast orbits) for both static and kinematic modes were also presented. The obtained results suggest that after a filter convergence period of 300 s, the point precision of the used E1/E5 combination and parameter estimation approach is at the cm-level for the horizontal components and at the dm-level for the height component. The accuracy estimates are at the low dm-level for the horizontal components and at the dm-level for the vertical one. Considering that broadcast orbits were used, that the number of visible satellites ranged from 5 to 6 and that no post-processing was done, we regard the results as promising.

In the next months, up to the completion of the ENCORE project, we plan on extending the simulation analysis to the whole scenario spectra, with and without a complete Galileo constellation, with and without GPS L1/L5 measurements, in static and kinematic modes, in real-time and post-processing modes, and with precision and broadcast orbits.

## 8. REFERENCES

- [1] Galileo, 2010, "European GNSS (Galileo) Open Service Signal-In-Space Interface Control Document". Galileo OS SIS ICD, Issue 1, February 2010
- [2] GPS Wing, 2010, "Navstar GPS Space Segment/User Segment L5 Interfaces". Interface Specification IS-GPS-705, Revision A, 8 June 2010.
- [3] GPS Wing, 2010, "Navstar GPS Space Segment/User Segment L1C Interface". Interface Specification IS-GPS-800, Revision A, 8 June 2010
- [4] Kouba, J., 2009, "A guide to using International GNSS Service (IGS) products". Technical Report, International GNSS Service. <http://acc.igs.org/UsingIGSProductsVer21.pdf>
- [5] Brazilian Law no. 10.267, of the 28th of August of 2001. Changes provisions of Laws 4.947, of the 6th of April 1966, 5.868, of the 12th of December of 1972, 6.015, of the 31st of December of 1973, 6.739, of the 5th of December of 1979, 9.393, of the 19th of December of 1996, and addresses other provisions. <http://www.planalto.gov.br>
- [6] Hein, G. W. *et al.*, 2006, "MBOC: The New Optimized Spreading Modulation Recommended for GALILEO L1OS and GPS L1C", Proceedings of IEEE/ION PLANS 2006, San Diego, California, USA. April 24-27, 2006.
- [7] Lestarquit, L. *et al.*, 2008. "AltBOC for Dummies or Everything You Always Wanted To Know About AltBOC". ION GNSS 2008, Savannah, GA, USA.
- [8] Sleewaegen, J.-M. *et al.*, 2004. "Galileo AltBOC Receiver". ENC GNSS 2004

- [9] I. Colomina *et al.*, 2011. “*The Accuracy Potential of Galileo E5/E1 pseudoranges for Surveying and Mapping*”, Proceedings of the ION GNSS 2011, Portland, Oregon.
- [10] INCRA 2010. “*Technical Norm for Geo-referencing of Rural Property*”, 2nd edition, Feb. 2010. [www.incra.gov.br](http://www.incra.gov.br)
- [11] Colomina, I., Blázquez, M., 2004. “*A unified approach to static and dynamic modelling in photogrammetry and remote sensing*”. International Archives of Photogrammetry, Remote Sensing and Spatial Information Sciences, Vol. 35-B1, Comm. I, pp. 178-183.
- [12] Goad, C., Yang, M., 1995. “*Precise GPS positioning in a mobile environment*”. Proceedings of the 1995 Mobile Mapping Symposium, Columbus, OH, USA.
- [13] O. Julien, C. Macabiau, 2007. “*1-Bit Processing of Composite BOC (CBOC) Signals and Extension to Time-Multiplexed BOC (TMBOC) Signals*”, ION NTM 2007, San Diego, CA.

## 9. ACKNOWLEDGEMENTS

The reported research has been conducted within the “Enhanced Code Galileo Receiver for Land Management in Brazil” (ENCORE) project funded by the European GNSS Supervisory Authority, in the frame of the 7th European Framework Program for Research and Development, FP7 (GSA contract no. 952708). The project runs from 2010 to 2012 and is realized by a European-Brazilian consortium lead by DEIMOS Engenharia (Portugal) and with participation of DEIMOS Space (Spain), the Institute of Geomatics (Spain), the Institute of Engineering Surveying and Space Geodesy of the University of Nottingham (UK), the São Paulo State University (UNESP, Brazil), OrbiSat da Amazônia (Brazil), Santiago e Cintra (Brazil) and MundoGeo (Brazil).

The development of the ENCORE receiver’s DSP core (FPGA) has also drawn benefits from the developments of the “Receptor de Código Híbrido para Navegação Urbana” RXURB project (Hybrid Code Receiver for Urban Navigation), funded under the Portuguese QREN initiative (IAPMEI contract no. 2010/12001).

The authors would also like to thank Mr. Régis Bueno from Geovector.